

DOI: 10.1002/cmdc.200700258

Antiproliferative Agents That Interfere with the Cell Cycle at the $G_1 \rightarrow S$ Transition: Further Development and Characterization of a Small Library of Stilbene-Derived Compounds

Daniela Pizzirani,^[a] Marinella Roberti,^{*[a]} Andrea Cavalli,^[a] Stefania Grimaudo,^[b] Antonietta Di Cristina,^[b] Rosaria Maria Pipitone,^[b] Nicola Gebbia,^[c] Manlio Tolomeo,^[b] and Maurizio Recanatini^[a]

In this continuation of our research on derivatives containing the stilbene privileged structure or that are derived from it, we report the results of further studies carried out on the previously initiated collection of compounds. We used a parallel synthetic approach to rapidly obtain small sets of compounds and started the annotation of the library in progress by calculating some physicochemical properties to be eventually correlated with biological activities. A pharmacophore for the antiproliferative activ-

ity was also built to summarize the features of the library. We evaluated the antiproliferative and pro-apoptotic activities of all compounds as well as the cell-cycle effects of some representative compounds. After in-depth investigations, 3'-phenyl-[1,1';4',1'']terphenyl-4,3'',5''-triol showed the most interesting biological profile, as it interferes with cell-cycle progression at the $G_1 \rightarrow S$ transition, acting on retinoblastoma phosphorylation and inducing cell differentiation.

Introduction

The cell cycle involves a series of events that occur in a cell from one mitotic division to the next. The transition from one phase of the cycle to another occurs in an orderly fashion and is regulated at several levels. Cell-cycle progression is controlled by specific checkpoints (G_1 and G_2), whereas cell-cycle entry is regulated by a restriction point, after which the cell is committed to proceed through the cycle toward division. A key molecule of this restriction point is the protein encoded by the tumor-suppressor gene retinoblastoma (*Rb*).^[1,2] The retinoblastoma protein (Rb) in its active state is hypophosphorylated and forms a complex with a group of transcription factors of the E2F family, thus blocking the cell cycle in the G_0 – G_1 phase. Following both partial phosphorylation by Cdk4–6/cyclin D and hyperphosphorylation by Cdk2/cyclin E, Rb releases E2F factors that activate the transcription of genes essential for the entry of the cell into the S phase, allowing $G_1 \rightarrow S$ transition and progression through the cycle. Loss of cell-cycle control is one of the hallmarks of neoplastic cells,^[3–5] and given these premises, the use of small organic molecules capable of targeting proteins related to cell-cycle control might represent an effective strategy for the development of innovative antitumor treatments.^[6]

Over the past years, we have been engaged in a project aimed at the discovery of either innovative antitumor lead candidates or chemical tools able to modulate specific molecular pathways of neoplastic cells. From a chemical point of view, we are particularly intrigued by privileged structures^[7] or molecular scaffolds that allow the parallel synthesis of natural-product-like derivatives. At present, the parallel procedure is suitable for rapidly obtaining variously substituted analogues,

particularly when a structure-based design strategy is not applicable owing to the lack of a specific target. For this reason, we were initially attracted by resveratrol (**1**, Figure 1), a stilbene-based apoptosis-inducing natural compound widely investigated for its chemopreventive and chemotherapeutic properties.^[8–11] Thus, following a parallel approach, we synthesized a small library of resveratrol-related *cis*- and *trans*-stilbene derivatives,^[12–15] in which a variety of substituents were introduced at positions 2', 3', 4', and 5' of the stilbene scaffold, and the 3,5-hydroxy groups were replaced by methoxy functions (Figure 1).

To increase the chemical diversity of our collection, we then prepared a second series of derivatives incorporating a phenyl ring as a bioisosteric substitution of the stilbene alkenyl

[a] Dr. D. Pizzirani, Prof. M. Roberti, Dr. A. Cavalli, Prof. M. Recanatini
Dipartimento di Scienze Farmaceutiche, Università di Bologna
Via Belmeloro 6, 40126 Bologna (Italy)
Fax: (+39) 051-209-9734
E-mail: marinella.roberti@unibo.it

[b] Dr. S. Grimaudo, Dr. A. Di Cristina, Dr. R. M. Pipitone, Dr. M. Tolomeo
Divisione di Ematologia e Servizio AIDS, Policlinico "P. Giaccone"
Via del Vespro 129, 90127 Palermo (Italy)

[c] Prof. N. Gebbia
Dipartimento di Oncologia, Policlinico "P. Giaccone", Università di Palermo
Via del Vespro 129, 90127 Palermo (Italy)

Supporting information for this article is available on the WWW under <http://www.chemmedchem.org> or from the author: general chemical methods; detailed biological protocols; synthesis of compounds **14**, **28**, **26**; physical and spectroscopic data for biphenyldimethoxy derivatives **9–13**, **33–35**, **33a**, terphenyl derivatives **17–25**, **17a–25a**, **31–32**, **31a**; and molecules used for the construction of the pharmacophore.

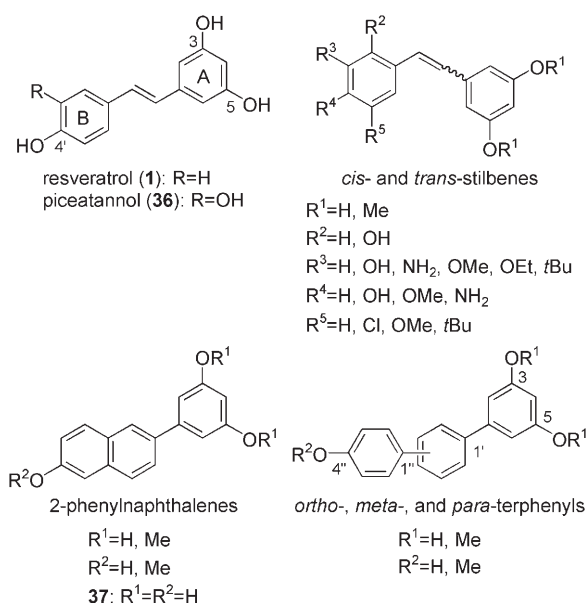


Figure 1. Stilbene-derived compounds.

bridge. We obtained both 2-phenylnaphthalenes and terphenyls, all of which presented the resveratrol-like pattern of oxygenated phenyl rings, i.e., one *para*-substituted and one *meta*-substituted phenyl group connected by an unsaturated/aromatic system (Figure 1).^[15] Among these derivatives, the trihydroxylated terphenyl **2** (for structure, see Table 1) showed the most peculiar biological profile. It caused a cell-cycle block at the G₀–G₁ phase, and remarkably, it was able to induce functional and morphological differentiation in HL60 cells. For these characteristics, we thought that **2** could be considered a promising lead to obtain small molecules capable of hitting targets related to cell-cycle control and inducing differentiation.

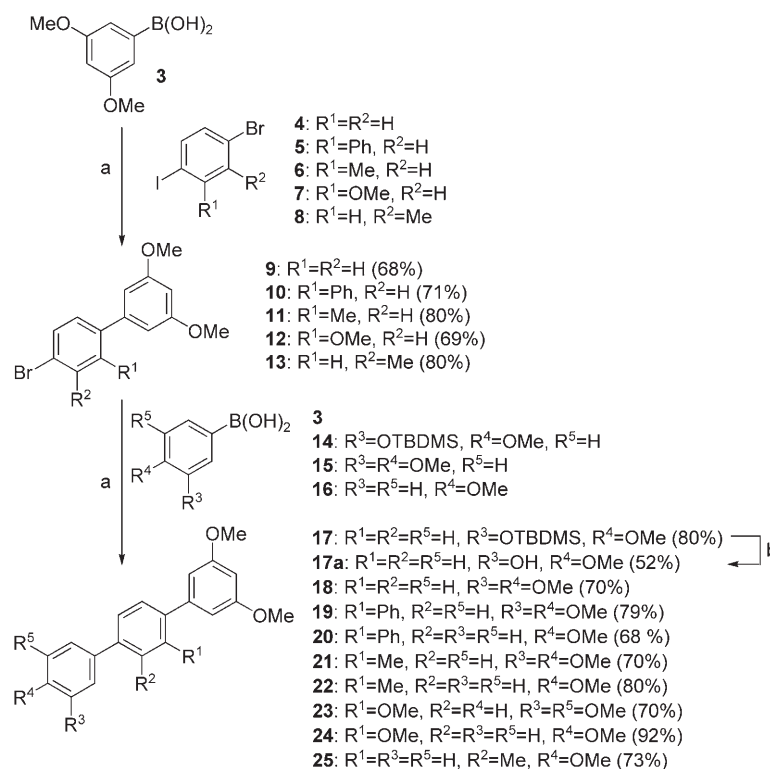
Continuing our studies, we describe herein the parallel synthesis of a further series of compounds including some variously substituted terphenyl derivatives and some biphenyl analogues. We thoroughly characterized all of the new derivatives with respect to their antiproliferative and pro-apoptotic activities, as well as their effects on cell cycle by carrying out experiments on HL60 and K562 (apoptosis-resistant) leukemia cell lines. Some of the compounds are active as apoptosis-inducing agents, and some

cause block of cells in the G₀–G₁ phase. Particularly, compound **20a** (Table 1) caused a marked increase in hypophosphorylated Rb and was also able to induce monocytic differentiation in HL60 cells.

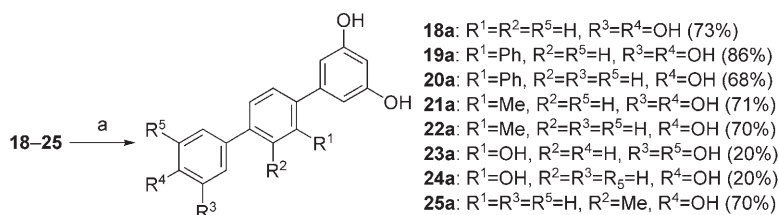
Finally, in an attempt to define the general stereoelectronic features of the library (present and previous series) and the SAR in relation to its antiproliferative activity, we calculated some physicochemical properties and built a pharmacophore summarizing the representative features of the whole collection of molecules.

Chemistry

The compounds were obtained following various parallel synthetic pathways (Schemes 1–3) carried out in a Carousel reaction station. The terphenyls **17–25** were obtained as shown in Scheme 1. A cross-coupling Suzuki reaction between 3,5-dimethoxyphenylboronic acid **3** and the appropriate 1-bromo-4-iodobenzene derivatives **4–8** in the presence of a catalytic amount of *tetrakis*-triphenylphosphine palladium gave the biphenyl dimethoxy derivatives **9–13**, respectively. A second Suzuki cross-coupling between compounds **9–13** and the appropriate boronic acids **3**, **14–16** provided terphenyls **17–25**. Removal of the *tert*-butyldimethylsilyl (TBDMS) group from derivative **17** using tetra-*N*-butylammonium fluoride (TBAF) afforded compound **17a**. Finally, the parallel demethylation of polymethoxy derivatives **18–25** with BBr₃ afforded the desired compounds **18a–25a** (Scheme 2).

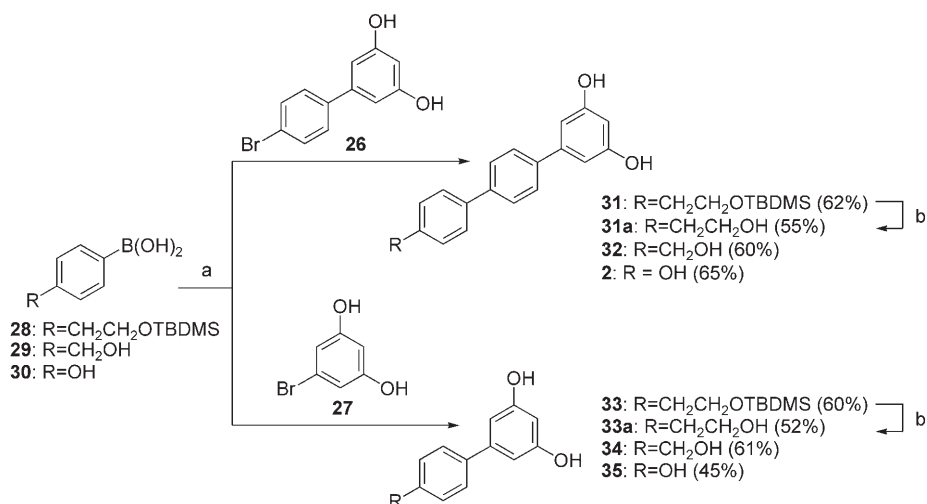


Scheme 1. Reagents and conditions: a) Pd(Ph₃P)₄, Na₂CO₃ (aq), toluene/EtOH (3:1), reflux, 5 h; b) TBAF, THF, room temperature, 3 h.



Scheme 2. Reagents and conditions: a) BBr₃, CH₂Cl₂, -78 °C, 18 h.

To synthesize terphenyls **31** and **32**, and biphenyls **33** and **34** that bear a hydroxy alkyl substituent, 4'-bromobiphenyl-3,5-diol **26** and 5-bromobenzene-1,3-diol **27** were used as halide components in the cross-coupling Suzuki reaction with the boronic acids **28** and **29**. Removal of the TBDMS protecting group from terphenyl **31** and biphenyl **33** using TBAF afforded compounds **31a** and **33a**, respectively. Moreover, the reaction of **26** and **27** with 4-hydroxyboronic acid **30** afforded the corresponding trihydroxyterphenyl **2** previously obtained by us through a different synthetic pathway,^[15] and trihydroxybiphenyl **35** (Scheme 3).



Scheme 3. Reagents and conditions: a) Pd(Ph₃P)₄, Na₂CO₃ (aq), toluene/EtOH (3:1), reflux, 5 h; b) TBAF, THF, room temperature, 3 h.

Biology

All compounds considered in this study were tested for their antiproliferative and pro-apoptotic activities on sensitive acute myelogenous leukemia HL60 cells and Bcr-Abl-expressing K562 cells. The antiproliferative activity of each compound was evaluated by counting cells with an automatic cell counter; apoptosis was evaluated by morphological assay and an annexin V test. The effects of compounds on the cell cycle were studied by flow cytometry after staining cells with propidium iodide.

For compound **20a**, which blocks cells in G₀-G₁ phase, we investigated the effects on Rb by flow cytometric analysis after incubation of K562 cells with anti-Rb or anti-hypophosphorylated Rb monoclonal antibodies (mAbs). To compare this activity with that of the previously obtained lead compound, the

same experiments were carried out with compound **2**. Moreover, we investigated the ability of **20a** to induce cell differentiation by evaluating the expression of CD61 and CD11c on HL60 cells.

Results

Biological action

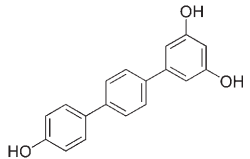
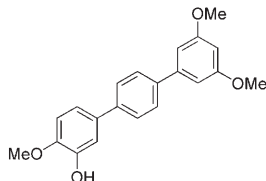
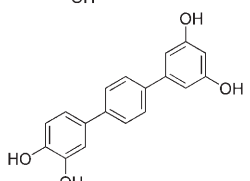
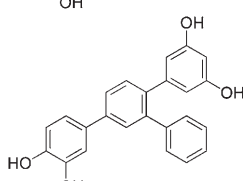
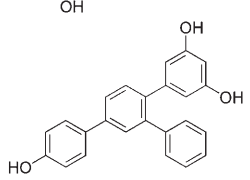
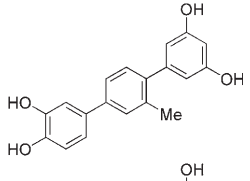
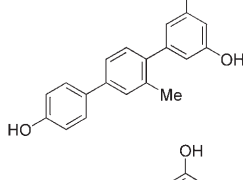
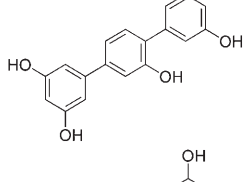
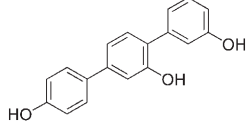
The antiproliferative and apoptosis-inducing activities of the new compounds are shown in Table 1, and these data are compared with those obtained with the reference terphenyl **2**.^[15] Antiproliferative and apoptosis-inducing activities were expressed as IC₅₀ (concentration inhibiting 50% of cell growth) and AC₅₀ (concentration inducing apoptosis in 50% of cells) values, respectively.

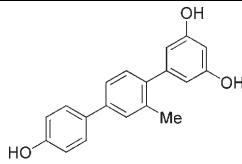
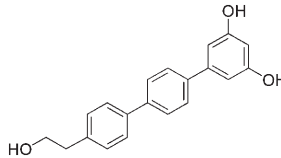
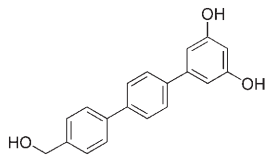
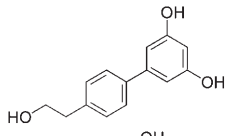
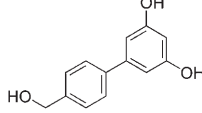
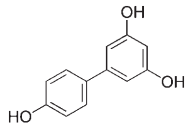
Within the terphenyl series, the antiproliferative and pro-apoptotic activities of compounds **18a**, **20a**, and **21a** on K562 cells were higher than the corresponding activities of the parent compound **2** on the same cell line, but they were lower on HL60 cells. The potency decreased on both HL60 and K562 cells for compounds lacking the 4''-hydroxy group: compound **23a**, as well as derivatives **31a** and **32**, in which the same hydroxy group was spaced by one (in **32**) or two (in **31a**) methylene units from the phenyl ring.

Despite their known antiproliferative effects in some cancer cell lines,^[16] all biphenyl derivatives showed IC₅₀ values above 80 μM in our tests. The effects of the most representative compounds **18a-22a** on cell cycle were evaluated in K562 cells by flow cytometry after staining cells with propidium iodide. In

Figure 2b-f, plots of the flow cytometric analyses of treated K562 cells are shown in comparison with the untreated cells (Figure 2a). Analysis of sub-G₀-G₁ (apoptotic peak), G₀-G₁, S, and G₂-M peaks reveal that the compounds studied elicit various effects on cell cycle, as shown in Table 2. Compounds **18a** and **21a** (Figure 2b and e, respectively) caused a decrease in the number of cells in the S phase and a moderate increase in the numbers of those in G₀-G₁ and G₂-M phases. In contrast, compounds **20a** and **22a** (Figure 2d and f, respectively) induced a block of cells in G₀-G₁ and a decrease in the percentage of cells in S and G₂-M phases. This effect was more evident if K562 cells were exposed to **20a**. Compound **19a** caused a decrease in the number of cells in G₂-M phase and a moderate increase of those in S phase (Figure 2c).

Table 1. Inhibitory and apoptosis-inducing activity of terphenyls **2**, **17 a–25 a**, **31 a**, **32** and biphenyls **33 a**, **34–35** in sensitive HL60 cells and in Bcr-Abl-expressing K562 cells.

Compound	HL60		K562		Clog P
	IC ₅₀ [μM] ± SE ^[a]	AC ₅₀ [μM] ± SE ^[b]	IC ₅₀ [μM] ± SE ^[a]	AC ₅₀ [μM] ± SE ^[b]	
2 	7.0 ± 1.2	25 ± 3	20 ± 2	75 ± 12	3.92
17 a 	> 80	> 80	> 80	> 80	5.11
18 a 	10 ± 1	38 ± 3	1.0 ± 0.2	50 ± 5	3.32
19 a 	20 ± 2	60 ± 8	22 ± 3	> 80	4.61
20 a 	30 ± 1	50 ± 5	8.0 ± 1.1	60 ± 7	5.21
21 a 	8.0 ± 0.9	55 ± 4	8.0 ± 0.9	60 ± 9	3.52
22 a 	10 ± 1	38 ± 4	20 ± 3	> 80	4.12
23 a 	> 80	> 80	> 80	> 80	2.28
24 a 	45 ± 6	> 80	12 ± 1	> 80	2.95

Compound	HL60		K562		ClogP
	IC ₅₀ [μM] ± SE ^[a]	AC ₅₀ [μM] ± SE ^[b]	IC ₅₀ [μM] ± SE ^[a]	AC ₅₀ [μM] ± SE ^[b]	
25a 	10 ± 1	60 ± 10	18 ± 2	> 80	4.12
31a 	> 80	> 80	> 80	> 80	3.77
32 	> 80	> 80	> 80	> 80	3.55
33a 	> 80	> 80	> 80	> 80	1.89
34 	> 80	> 80	> 80	> 80	1.66
35 	> 80	> 80	> 80	> 80	2.03

[a] Concentration at which 50% cell growth is blocked. [b] Concentration at which apoptosis is induced in 50% of the cells.

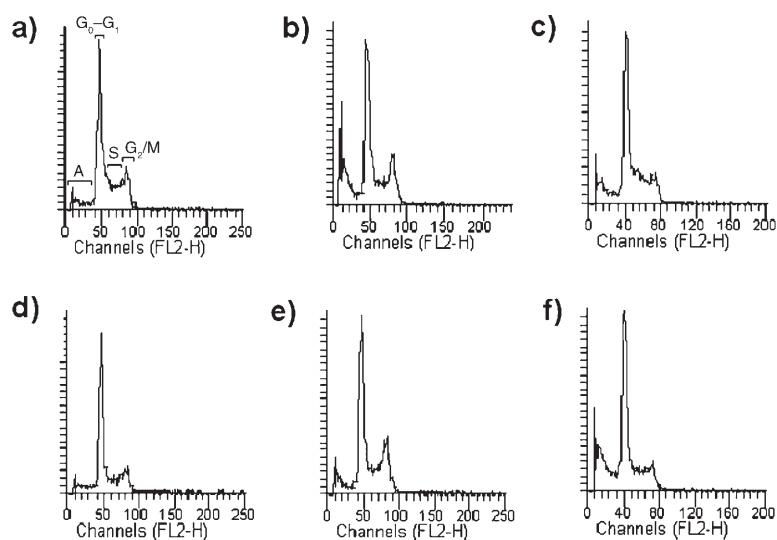


Figure 2. Effects of compounds **18a**, **19a**, **20a**, **21a**, and **22a** on DNA content per cell following the treatment of K562 cells for 24 h. The cells were cultured a) without compounds, or with each compound used at the following concentrations: b) **18a**, 40 μM; c) **19a**, 60 μM; d) **20a**, 40 μM; e) **21a**, 40 μM; f) **22a**, 60 μM. Cell-cycle distribution was analyzed by the standard propidium iodide procedure as described in the Supporting Information and correlates with the data listed in Table 2. Sub-G₀-G₁ (A), G₀-G₁, S, and G₂-M cells are indicated in panel a).

Given the relevance of the block of cells in G₀-G₁ phase, this action of **20a** was studied in greater detail by investigating its effects on the phosphorylation of Rb in the Bcr-Abl-expressing K562 cells. As shown in Figure 3, **20a** caused a marked increase of hypophosphorylated Rb, while the total amount of Rb was similar to that of untreated cells. Considering that the parent compound **2** was also able to induce a stable block in G₀-G₁ phase,^[15] we compared the effects of **20a** on Rb with those of **2**. Unlike **20a**, compound **2** caused a decrease in total Rb without affecting the levels of hypophosphorylated Rb (Figure 3). Additionally, as Rb

Table 2. Effects of terphenyl derivatives **18a–22a** on cell-cycle distribution in K562 cells.^[a]

Treatment	Cells in phase: [%]		
	G ₀ –G ₁	S	G ₂ –M
None	46	41	13
18a ^[b]	51	33	16
19a ^[c]	46	47	7
20a ^[b]	61	27	12
21a ^[b]	50	31	19
22a ^[c]	57	38	5

[a] Correlate with Figure 2. [b] 40 μM . [c] 60 μM .**Physicochemical characteristics and pharmacophore definition**

In an attempt to rationalize the SAR regarding the antiproliferative activity of the whole library (this study and references [12, 13, 15]), we calculated some physicochemical properties of the most representative compounds and looked for correlations with the IC₅₀ data. The partition coefficient ($\log P$) was calculated (Bio-Loom version 1.0, 2006, BioByte Corp., Claremont, CA, USA) for the whole collection of 50 molecules (data not shown), and the values for the compounds reported herein are shown in Table 1. The average $\log P$ value is 4.21 ($s=1.71$),

which reflects the rather high lipophilicity of this class of polycyclic compounds, with a minimum of 2.24 (piceatannol (**36**), Figure 1) and a maximum of 7.63 (compound **3h** in reference [9]). Although the rather high average value is mostly due to the value of >7 for only three stilbene analogues substituted with bulky protecting groups, the range of lipophilicity is consistent with the general ability of these derivatives to easily penetrate the cell membrane; compounds with $\log P$ values at the higher end of the range may have some pharmacokinetic problems in cases of in vivo administration. Considering the biological activities reported in Table 1 and previously,^[12, 15] we found no significant correlation between potency and $\log P$.

Given the presence of the extended aromatic systems that characterize the compounds under study, we evaluated some properties related to the electron distribution over the molecules. In this case, we focused on compounds that carry a structural pattern reminiscent of our starting lead resveratrol (**1**), i.e., an extended “*trans*-like” conjugated skeleton substituted with OH groups in positions corresponding to 3, 5, and 4’ of resveratrol. We then calculated frontier orbital (HOMO and LUMO) energies, partial atomic charges, and molecular electrostatic potentials (MEPs) for compounds **1**, **2**, **18a**, **20a**, **36**, and **37** (trihydroxyphenylnaphthalene, Figure 1). In Table 3, the frontier orbital energies and HOMO–LUMO differences of these compounds are reported together with their antiproliferative potencies. Again, no significant trend was observed between activity and physicochemical properties. Similarly, the consider-

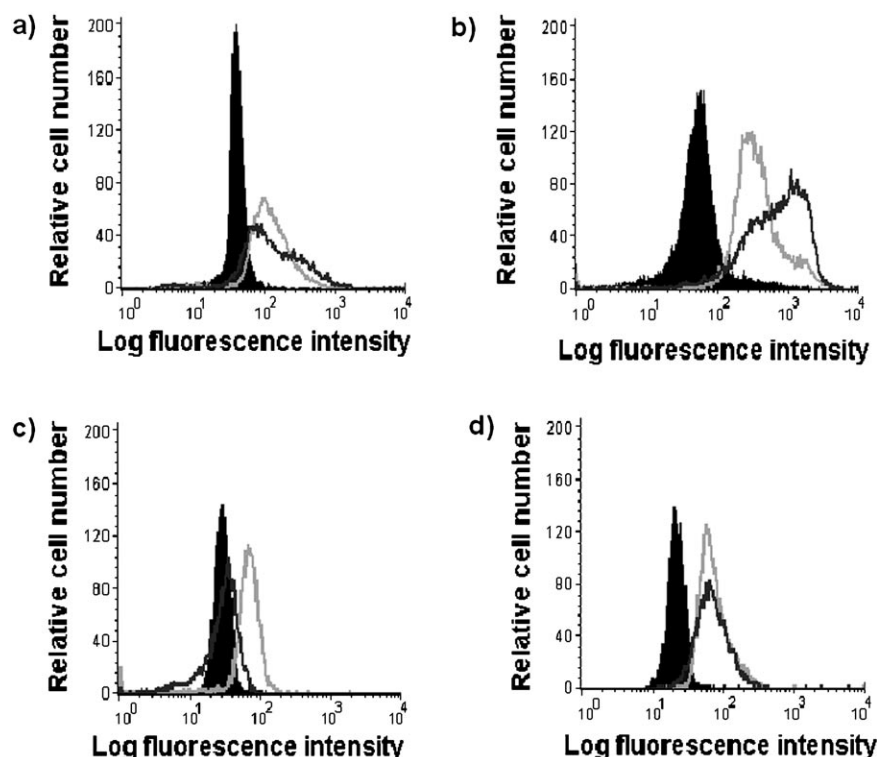


Figure 3. Effects of compounds **20a** and **2** on total Rb and hypophosphorylated Rb expression evaluated by flow cytometry after staining K562 cells with a fluorescein isothiocyanate (FITC)-conjugated anti-Rb mAb, or a phycoerythrin (PE)-conjugated mAb raised against hypophosphorylated Rb. a) Expression of total Rb in cells treated with (dark-gray line) or without (light-gray line) 60 μM **20a**. b) Expression of hypophosphorylated Rb in cells treated with (dark-gray line) or without (light-gray line) 60 μM **20a**. c) Expression of total Rb in cells treated with (dark-gray line) or without (light-gray line) 60 μM **2**. d) Expression of hypophosphorylated Rb in cells treated with (dark-gray line) or without (light-gray line) 60 μM **2**. Black area-filled curves: cells stained with an isotype mAb (control).

also plays an important role in cell differentiation, and **20a** is able to modify the phosphorylation state of Rb, we investigated its potential differentiating activity in HL60 cells. Cells were exposed to **20a** at 10 μM , and after 72 h the expression of CD61 (monocytic marker) and CD11c (granulocytic marker) were evaluated by flow cytometry. As shown in Figure 4, cells exposed to **20a** increased their expression of CD61, indicating that this compound is able to induce monocytic differentiation.

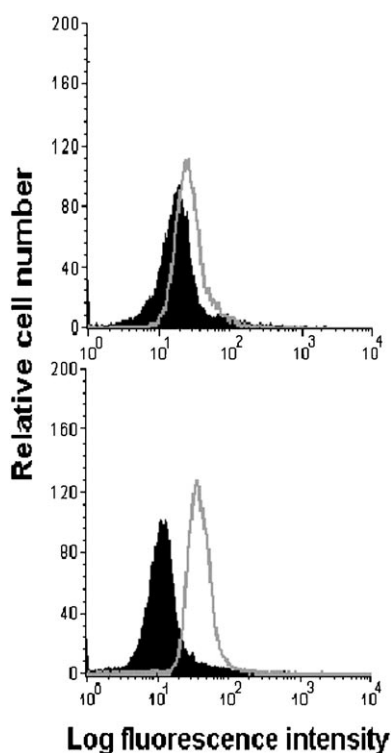


Figure 4. Expression of CD11c (top panel) and CD61 (bottom panel) differentiation markers in HL60 cells cultured for 5 days without (black area-filled curves) or with (gray lines) 10 μM **20a**.

ation of partial atomic charges and MEPs (not shown) did not reveal any link with the variations in potency.

Finally, to summarize the SAR features of the entire collection of molecules synthesized and tested in the project, we built a pharmacophore by means of the GALAHAD program (SYBYL version 7.3, 2006, Tripos Inc., St. Louis, MO, USA). To this end, a small number (seven) of potent to moderately potent molecules was selected that span all the different skeletons represented in the library, i.e., *trans*- and *cis*-stilbenes, *ortho*-, *meta*-, and *para*-terphenyls, and 2-phenylnaphthalenes (Figure 1 SI). Among all of the solutions proposed by the program, one was accepted that allowed a meaningful alignment of all the other derivatives.

The pharmacophore is shown in Figure 5a, where the stereoelectronic features are displayed as spheres, the sizes of which are inversely proportional to the spatial definition of the property. The core of the pharmacophoric scheme is formed by four hydrophobic features (HY) that derive from the shape of the two chemotypes considered in this collection of molecules, exemplified by *trans*- and *cis*-resveratrol, or correspondingly, *para*- and *ortho*-terphenyls. The AA and DA spheres represent the H-bond acceptor and donor groups, respectively, that decorate the phenyl rings of most molecules of the series. In some cases, the acceptor and donor features are overlapped, indicating the presence of an OH function. To illustrate how the most representative molecules of the collection match the pharmacophoric features, the compounds resveratrol (**1**), **2**, and **20a** are shown superimposed onto the pharma-

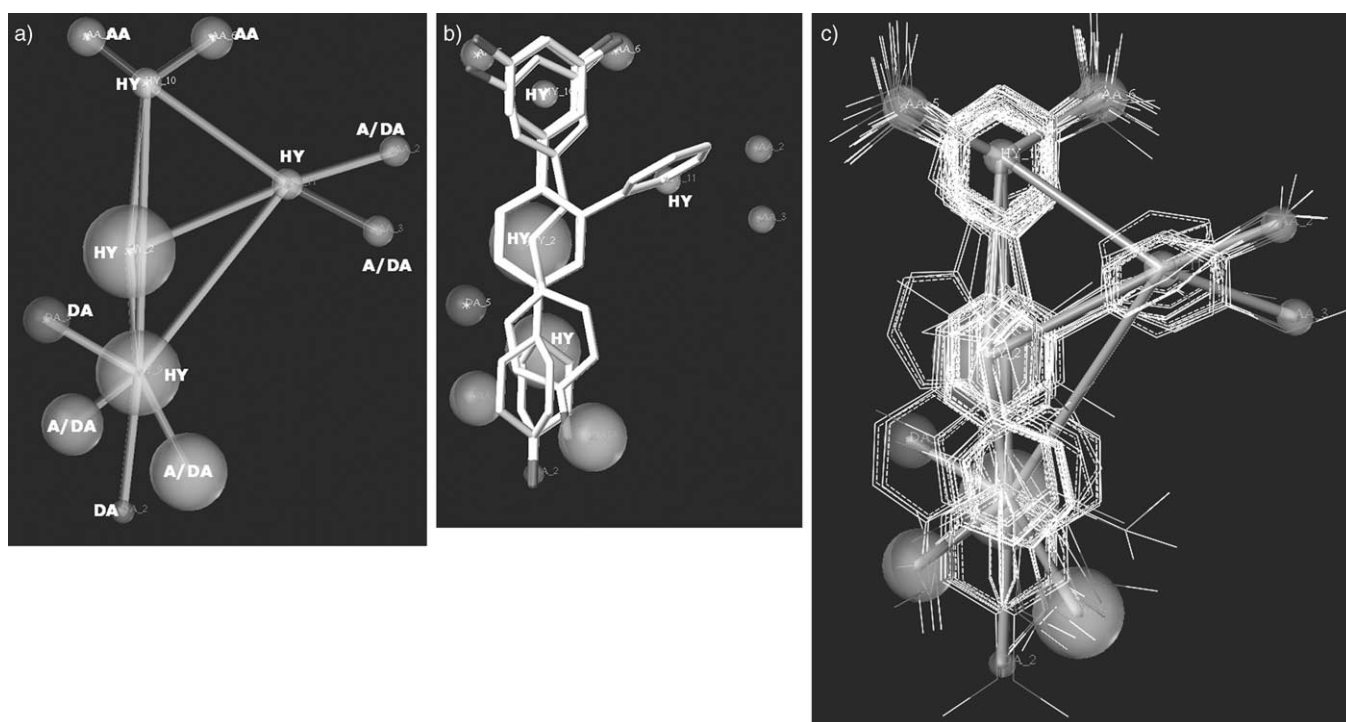
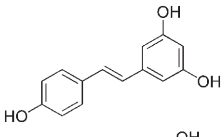
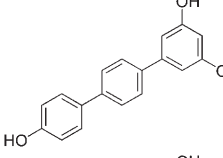
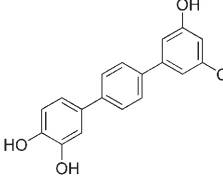
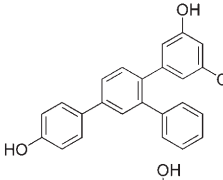
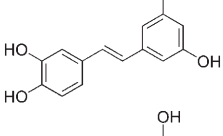
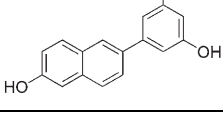


Figure 5. a) The selected GALAHAD pharmacophore is displayed as a collection of features (spheres representing the spatial tolerance) connected by dummy bonds. Feature types are indicated: HY = hydrophobic features, DA = H-bond donor atoms, AA = H-bond acceptor atoms, and A/DA = overlay of acceptor and donor atom features. b) Compounds **1** (a *trans*-stilbene), **2** (a *para*-terphenyl), and **20a** (a 2'-phenyl-*para*-terphenyl) aligned onto the pharmacophore showing the correspondence of the hydrophobic features with the hydrophobic scaffolds of the main chemotypes of the collection (the smaller the sphere shape, the more precise the alignment). c) Alignment of all molecules of the library onto the GALAHAD pharmacophore.

Table 3. Frontier orbital energies of compounds **1**, **2**, **18a**, **20a**, **36**, and **37**. Antiproliferative IC₅₀ values in HL60 and K562 cells of the same compounds are also reported.

Compound	E_{HOMO} [eV]	E_{LUMO} [eV]	$\Delta\text{HOMO-LUMO}$	IC ₅₀ [$\mu\text{M} \pm \text{SE}$]	
				HL60	K562
1 	5.2546372	-1.210934	4.0437032	5.0 ± 0.8 ^[a]	28 ± 2 ^[a]
2 	5.5000894	-0.8960912	4.6039982	7.0 ± 1.2 ^[a]	20 ± 2 ^[a]
18a 	5.3836221	-0.9339158	4.4497063	10 ± 1	1.0 ± 0.2
20a 	5.5145118	-0.857178	4.6573338	30 ± 1	8.0 ± 1.1
36 	5.1640212	-1.2343363	3.9296849	10 ± 3 ^[b]	22 ± 4 ^[b]
37 	5.4573666	-1.0648056	4.392561	28 ± 4 ^[a]	20 ± 4 ^[a]

[a] Ref. [15]. [b] Ref. [14].

cophoric frame in Figure 5b. In Figure 5c, all the molecules of the collection are aligned onto the pharmacophoric scheme, showing how it accounts for the general stereoelectronic features of the series.

Discussion

Antiproliferative action and interference with cell-cycle progression

The peculiar biological profile shown by the previously described trihydroxylated terphenyl derivative **2**^[15] prompted us to continue our studies on this class of compounds. Following a parallel approach taking advantage of a Suzuki cross-coupling protocol, we synthesized variously substituted terphenyl derivatives and some biphenyl analogues.

Among the terphenyl derivatives described herein, three compounds (**18a**, **20a**, and **21a**) showed an interesting higher cytotoxic activity in apoptosis-resistant K562 cells than in apoptosis-sensitive HL60 cells, and one of them, **20a**, was able to block Bcr-Abl-expressing K562 cells in the G₀-G₁ phase of

the cell cycle. From the data listed in Table 1, it appears that structural variations are tolerated only if the terphenyl scaffold, eventually substituted with oxygenated functions, is preserved. In fact, biphenyls (even **35**, showing the same OH substitution pattern as **2**) as well as compounds **31a** and **32** (in which the 4''-OH function is linked to the phenyl ring through a mono- or bis-methylene bridge, respectively) were devoid of significant antiproliferative and pro-apoptotic activities. Indeed, from both the previous and the present work on the library of compounds developed to date, **20a** and **2** emerge as the compounds with the most intriguing biological profile.

Comparing the activity of **20a** with that of **2**, we observed that the former is endowed with higher pro-apoptotic activity and is able to induce a more marked G₀-G₁ block. Moreover, the flow cytometry assay of total and hypophosphorylated Rb expression in K562 cells showed that **20a** induces a marked increase in the hypophosphorylated form of Rb without any modification to the total Rb level. In contrast, the parent compound **2**, which was similarly able to induce a stable block in G₀-G₁ phase, caused a decrease in total Rb without affecting the levels of hypophosphorylated Rb. This is consistent with a

relative decrease in phosphorylated Rb and a corresponding increase in hypophosphorylated Rb, and suggests that compound **2** might act not simply by interfering with Rb phosphorylation at the G₁-S checkpoint, but through a different mechanism.

The key proteins involved in the cell cycle and its control are most commonly altered in human cancers.^[3-5] Two major control pathways of cellular progression from G₁ to S phase originate from different stimuli, such as TGFβ (following the p16INK4A, Cdk4-6/cyclin D pathway) and DNA damage (following the p53, p21Waf1, Cdk2/cyclin E pathway), but both converge onto Rb, which acts as a common link between the pathways and is pivotal in controlling the checkpoint. Mutations in the *Rb* gene have been described in a wide variety of neoplasms, and constitutive phosphorylation/inactivation of Rb has been implicated in conferring uncontrolled growth to many cancer cells.^[17] Currently, phosphorylation of Rb is the key molecular event that regulates the checkpoint passage, allowing or preventing E2F transcription factor release and the expression of S-phase genes. If the action of **20a** results in an increase of hypophosphorylated Rb, it can be hypothesized that it interferes with some upstream pathways that regulate Rb phosphorylation, such as the expression, action, and inhibition of Cdk4-6 or Cdk2, or others. On the other hand, the decrease of total Rb following exposure of K562 cells to compound **2** might tentatively be interpreted as a result of degradation of phosphorylated Rb. A similar activity was recently described for the typhostin AG1024 in melanoma cells.^[18] This compound caused the loss of phosphorylated forms of Rb that was not associated with suppression of Cdk2 or Cdk4 activity, but rather with proteasomal and non-proteasomal degradation of phosphorylated Rb. However, whereas the MDM2-mediated ubiquitin-dependent degradation of hypophosphorylated Rb is rather well known,^[19,20] less is known about proteasome-mediated Rb degradation. In the case of the tyrosine kinase inhibitor AG1024, this action is associated with a decrease in Bcr-Abl expression in K562 cells and a delay of tumor growth in a mouse model,^[21] making this compound a promising candidate for clinical use. Experiments are under way to elucidate the profile of compound **2** in this direction.

Although compounds **20a** and **2** act through different mechanisms on Rb, both caused an arrest of the G₁→S transition and cell differentiation. However, in contrast to compound **20a**, compound **2** was able to induce both cell-surface-marker differentiation and morphological differentiation. At present, we do not have enough data to determine whether or not the higher differentiating activity of compound **2** with respect to compound **20a** is correlated with the different activity toward Rb. Even though it is well known that Rb is involved in cell differentiation in addition to playing a role in the control of the G₁→S transition,^[22] more in-depth studies are required to understand the mechanism(s) of the potent differentiating activity of compound **2**.

Pharmacophore and library features

The exploration of calculated physicochemical properties such as partition coefficients, frontier orbital energies, partial atomic charges, and MEPs did not result in the identification of quantitative correlations between activity and properties. However, this is not unusual for a series of compounds that do not originate from a biological lead, but are instead purposely assembled to span the chemical space in the search of a lead. For instance, from several QSAR reports on pro-apoptotic^[23,24] or anticancer activity,^[25,26] a clear understanding of the physicochemical properties involved in eliciting such effects has not yet emerged. It seems that the complexity of the mechanisms and the likely high number of targets possibly implicated prevent easy identification of the key determinants, especially if the training sets are small. On the other hand, regarding the role of electronic descriptors, the LUMO energies have sometimes been correlated with the mutagenic effect of aromatic compounds (HOMO energies were much less frequently involved), and this might be ascribed to the electrophilic nature of most mutagens that express their toxicity by reacting with the nucleophilic DNA.^[27] The ΔHOMO-LUMO parameter has been proposed as a descriptor of the photoinduced toxicity of some polyaromatic compounds.^[28,29] However, in the present case, no hints emerged as to the possible involvement of reactive species in the mechanism of cytotoxicity of some of the compounds tested.

A more general approach to summarizing the SAR for the antiproliferative properties of the library was attempted with the construction of the pharmacophoric scheme shown in Figure 5. The pharmacophore is based on the most active compounds (in terms of IC₅₀) and illustrates quite generally the main structural features responsible for the cytotoxicity against HL60 and K562 cells. In this sense, it can be considered as biased, i.e., it reflects the structure of the most potent compounds that belong to both the main scaffolds included in the collection of molecules (stilbenes and terphenyls), and will be used as a query in virtual screening experiments aimed at the identification of novel chemotypes endowed with antiproliferative activity.

As a final observation, the present physicochemical characterization of the whole collection of compounds might be considered as a first step towards an extended annotation of the collection both in physicochemical and in biological terms. Indeed, besides increasing the size of the library, the determination of the biological properties and the calculation of physicochemical descriptors of all the compounds included is crucial to permit the exploitation of the same library in different biological contexts.

Conclusions

In this continuation of our research on derivatives containing the stilbene privileged structure or derived from it, we report the results of some further studies carried out on the previously initiated collection of compounds. We took advantage of the parallel synthetic approach that proved to be efficient to

rapidly obtain small sets of compounds, and appropriate when random substitutions have to be explored in the lack of either a specific target or a clearly defined SAR pattern. Moreover, we started the annotation of the library in progress by calculating some physicochemical features to be eventually correlated with biological properties. A pharmacophore for the antiproliferative activity was then built in view of its use in virtual screening experiments aimed at increasing the chemical diversity of the collection.

From a biological point of view, considering the whole library, two compounds (**20a** and **2**) emerged as those endowed so far with the most interesting profiles in terms of their ability to interfere with cell-cycle progression. Although the mechanisms by which compounds **20a** and **2** cause, respectively, a block of Rb phosphorylation and a degradation of phosphorylated Rb are still unknown, it is reasonable to suppose that these compounds might have interesting implications for cancer therapy. In fact, drugs that are able to block and/or kill cancer cells in G_0 – G_1 phase are currently considered of interest, because most chemotherapeutic drugs available for the treatment of malignancies act in the S or G_2 –M phase of the cell cycle, but not in G_0 – G_1 , thus allowing a variable percentage of cells in G_0 – G_1 phase to escape from the cytotoxic effects of the therapy. This and the need to explore the molecular mechanism of compounds that are able to interfere with cell-cycle progression justifies further research focused on Rb and block of the G_1 →S transition.

Experimental Section

General parallel procedure for the synthesis of biphenyls 9–13 and 33–35

In distinct reactors, *p*-iodobromobenzenes **4–8** and 3,5-dihydroxybromobenzene **27** (1.0 equiv) were dissolved in toluene (10 mL). Boronic acids **3**, **28–30** (2 equiv) in EtOH (3 mL) and Na_2CO_3 (2 M, aq, 3.0 equiv) were then added to the corresponding reactors (Schemes 1 and 3), and the resulting mixtures were deoxygenated with a stream of N_2 . After 10 min, $\text{Pd}(\text{PPh}_3)_4$ (0.05 equiv) was added, and each mixture was brought to reflux and allowed to stir under N_2 for 5 h, then cooled to room temperature and treated as follows: Each solution was poured into a mixture of H_2O and Et_2O , and the two phases were separated. The aqueous layer was washed with Et_2O , and the organic phases were combined and washed with 1 M NaOH followed by brine. The ether solution was dried over Na_2SO_4 and evaporated. Purification of each crude product by flash chromatography using petroleum ether/ethyl acetate yielded the corresponding 3,5-dimethoxybiphenyl derivatives **9–13** and the 3,5-dihydroxybiphenyl derivatives **33–35**.

General parallel procedure for the synthesis of terphenyl derivatives 17–25, 31–32, and 2

Each of the bromobiphenyldimethoxy derivatives **9–13** and bromobiphenyldihydroxy derivative **26** (2.0 equiv) were dissolved in toluene (20 mL) in distinct reactors. Various substituted phenylboronic acids **3**, **14–16**, or **28–30** (2 equiv) in EtOH (3 mL), and aqueous Na_2CO_3 (2 M, 3.0 equiv) were added to distinct reactors containing the corresponding brominated derivatives **9–13** and **20** (Schemes 1 and 3), and the resulting 12 mixtures were deoxygenated with a

stream of N_2 . After 10 min, $\text{Pd}(\text{PPh}_3)_4$ (0.05 equiv) was added, and each mixture was brought to reflux and allowed to stir under N_2 for 3–12 h, then cooled to room temperature and treated as follows: Each solution was poured into a mixture of H_2O and Et_2O , and the two phases were separated. The aqueous layer was washed with Et_2O , and the organic phases were combined and washed with 1 M NaOH followed by brine. The ether solution was dried over Na_2SO_4 and evaporated. Purification of each crude product by flash chromatography using petroleum ether/ethyl acetate yielded the corresponding terphenyl derivatives **17–25**, **31–32**, and **2**.

General parallel procedure for demethylation to polyhydroxyterphenyl derivatives 18a–25a

In eight distinct reactors, the polymethoxy derivatives **18–25** (1 equiv) were dissolved in anhydrous CH_2Cl_2 (10 mL) at -78°C . BBr_3 (1 M in CH_2Cl_2 , 1 equiv for each methoxy group to cleave) was then added to each solution (Scheme 2), and the resulting reaction mixture was allowed to warm to room temperature for 20 h, then cooled at 0°C and treated as follows: Each solution was poured into H_2O , and the two phases were separated. The aqueous layer was washed twice with CH_2Cl_2 , and the organic phases were combined and washed with a solution of sodium thiosulfate (1 M) followed by H_2O . The organic layer was dried over Na_2SO_4 and evaporated to dryness. Purification of each crude product by flash chromatography using petroleum ether/ethyl acetate yielded the corresponding polyhydroxy derivatives **18a–25a**.

Computational methods

The seven parent molecules representative of each scaffold (*cis*- and *trans*-stilbene, *ortho*-, *meta*-, and *para*-terphenyl, 2'-phenyl-*para*-terphenyl, and 2-phenylnaphthalene) were first built in SYBYL 7.3 (Tripos Inc., 2006, St. Louis, MO, USA) and then geometry optimized through the conjugate gradient method. Subsequently, all molecules were submitted to Monte Carlo conformational analysis with MacroModel 9.0 (Schrödinger Inc., 2005 Portland, OR, USA), and conformers were energy minimized with MMFF94s^[30,31] force field as implemented in SYBYL 7.3. All the molecules of the collection were then built by adding the corresponding substituents onto the basic scaffolds and minimizing the resulting structures.

The frontier orbitals, partial atomic charges, and MEPs of compounds **1**, **2**, **18a**, **20a**, **36**, and **37** were calculated at the B3LYP/6-31G* level of theory after minimization using the Gaussian 03 software (Gaussian Inc., 2003, Pittsburgh, PA, USA).

The pharmacophore was built with the GALAHAD program of SYBYL 7.3. GALAHAD aligns molecules and generates pharmacophore hypotheses in the form of hypermolecules incorporating the structural information of the dataset.^[32,33] The core computational methodology of GALAHAD is a genetic algorithm that operates on a set of individual models in which each model is defined by a set of torsions for each molecule in the dataset. The pharmacophore is obtained through a procedure whereby the program first identifies corresponding features in ligands paired on the basis of structural similarity, then aligns the conformations in Cartesian space and merges the ligands into a single hypermolecule. The procedure is repeated until all of the molecules are incorporated in the master hypermolecule. The models generated by GALAHAD represent a tradeoff among the conflicting demands of maximizing pharmacophore and steric consensus, and minimizing energy. In the present case, the most potent molecules (antiproliferative activity) for each

scaffold were chosen (Figure 1 S1), and from this dataset, 20 pharmacophoric hypotheses were generated using the default parameters of GALAHAD. All the other molecules of the collection were then aligned using each pharmacophore as a template, and the best pharmacophore was selected as the one that allowed the most reasonable overall alignment.

Acknowledgements

This work was supported by a PRIN2006 Project Grant from MiUR, Italy.

Keywords: antitumor agents · C–C coupling · cell cycle · pharmacophores

- [1] C. Giacinti, A. Giordano, *Oncogene* **2006**, *25*, 5220–5227.
- [2] L. Khidr, P. L. Chen, *Oncogene* **2006**, *25*, 5210–5219.
- [3] K. Vermeulen, D. R. Van Bockstaele, Z. N. Berneman, *Cell Proliferation* **2003**, *36*, 131–149.
- [4] C. Sandhu, J. Slingerland, *Cancer Detect. Prev.* **2000**, *24*, 107–118.
- [5] M. Hall, G. Peters, *Adv. Cancer Res.* **1996**, *68*, 67–108.
- [6] G. K. Schwartz, M. A. Shah, *J. Clin. Oncol.* **2005**, *23*, 9408–9421.
- [7] R. Breinbauer, I. R. Vetter, H. Waldmann, *Angew. Chem.* **2002**, *114*, 3002–3015; *Angew. Chem. Int. Ed.* **2002**, *41*, 2878–2890.
- [8] M. Athar, J. H. Back, X. Tang, K. H. Kim, L. Kopelovich, D. R. Bickers, A. L. Kim, *Toxicol. Appl. Pharmacol.* **2007**, *224*, 274–283.
- [9] J. A. Baur, D. A. Sinclair, *Nat. Rev. Drug Discovery* **2006**, *5*, 493–506.
- [10] M. Jang, L. Cai, G. O. Udeani, K. V. Slowing, C. F. Thomas, C. W. Beecher, H. H. Fong, N. R. Farnsworth, A. D. Kinghorn, R. G. Mehta, R. C. Moon, J. M. Pezzuto, *Science* **1997**, *275*, 218–220.
- [11] C. Cal, H. Garban, A. Jazirehi, C. Yeh, Y. Mizutani, B. Bonavida, *Curr. Med. Chem. Anti-Cancer Agents* **2003**, *3*, 77–93.
- [12] M. Roberti, D. Pizzirani, D. Simoni, R. Rondanin, R. Baruchello, C. Bonora, F. Buscemi, S. Grimaudo, M. Tolomeo, *J. Med. Chem.* **2003**, *46*, 3546–3554.
- [13] R. Amorati, M. Lucarini, V. Mugnaini, G. F. Pedulli, M. Roberti, D. Pizzirani, *J. Org. Chem.* **2004**, *69*, 7101–7107.
- [14] M. Tolomeo, S. Grimaudo, A. Di Cristina, M. Roberti, D. Pizzirani, M. Meli, L. Dusonchet, N. Gebbia, V. Abbadessa, L. Crosta, R. Barucchello, G. Grisolia, F. Invidiata, D. Simoni, *Int. J. Biochem. Cell Biol.* **2005**, *37*, 1709–1726.
- [15] M. Roberti, D. Pizzirani, M. Recanatini, D. Simoni, S. Grimaudo, A. Di Cristina, V. Abbadessa, N. Gebbia, M. Tolomeo, *J. Med. Chem.* **2006**, *49*, 3012–3018.
- [16] M. Pisano, G. Pagnan, M. Loi, M. E. Mura, M. G. Tilocca, G. Palmieri, D. Fabbri, M. A. Dettori, G. Delogu, M. Ponzoni, C. Rozzo, *Mol. Cancer* **2007**, *6*, 8.
- [17] J. R. Nevins, *Hum. Mol. Genet.* **2001**, *10*, 699–703.
- [18] M. von Willebrand, E. Zacksenhaus, E. Cheng, P. Glazer, R. Halaban, *Cancer Res.* **2003**, *63*, 1420–1429.
- [19] C. Uchida, S. Miwa, K. Kitagawa, T. Hattori, T. Isobe, S. Otani, T. Oda, H. Sugimura, T. Kamijo, K. Ookawa, H. Yasuda, M. Kitagawa, *EMBO J.* **2005**, *24*, 160–169.
- [20] S. Miwa, C. Uchida, K. Kitagawa, T. Hattori, T. Oda, H. Sugimura, H. Yasuda, H. Nakamura, K. Chida, M. Kitagawa, *Biochem. Biophys. Res. Commun.* **2006**, *340*, 54–61.
- [21] E. Deutsch, L. Maggiorella, B. Wen, M. L. Bonnet, K. Khanfir, V. Frascogna, A. G. Turhan, J. Bourhis, *Br. J. Cancer* **2004**, *91*, 1735–1741.
- [22] W. Du, J. Pogoriler, *Oncogene* **2006**, *25*, 5190–5200.
- [23] C. Hansch, A. Jazirehi, S. B. Mekarpati, R. Garg, B. Bonavida, *Bioorg. Med. Chem.* **2003**, *11*, 3015–3019.
- [24] C. D. Selassie, S. Kapur, R. P. Verma, M. Rosario, *J. Med. Chem.* **2005**, *48*, 7234–7242.
- [25] S. B. Mekarpati, W. A. Denny, A. Kurup, C. Hansch, *Bioorg. Med. Chem.* **2001**, *9*, 2757–2762.
- [26] R. Garg, W. A. Denny, C. Hansch, *Bioorg. Med. Chem.* **2000**, *8*, 1835–1839.
- [27] K. Tuppurainen, *Chemosphere* **1999**, *38*, 3015–3030.
- [28] O. G. Mekenyan, G. T. Ankley, G. D. Veith, D. J. Call, *Chemosphere* **1994**, *28*, 567–582.
- [29] M. Grote, G. Schuurmann, R. Altenburger, *Environ. Sci. Technol.* **2005**, *39*, 4141–4149.
- [30] T. A. Halgren, *J. Comput. Chem.* **1996**, *17*, 490–519.
- [31] T. A. Halgren, *J. Comput. Chem.* **1999**, *20*, 720–729.
- [32] N. J. Richmond, C. A. Abrams, P. R. Wolohan, E. Abrahamian, P. Willett, R. D. Clark, *J. Comput.-Aided Mol. Des.* **2006**, *20*, 567–587.
- [33] J. K. Shepphird, R. D. Clark, *J. Comput.-Aided Mol. Des.* **2006**, *20*, 763–771.

Received: September 18, 2007

Revised: November 2, 2007

Published online on December 27, 2007